THE JOURNAL OF BIOLOGICAL CHEMISTRY VOL. 287, NO. 11, pp. 8154–8162, March 9, 2012

Pyroglutamate Amyloid β (Aβ) Aggravates Behavioral Deficits in Transgenic Amyloid Mouse Model for Alzheimer Disease[S]

Received for publication, September 28, 2011, and in revised form, January 18, 2012 Published, JBC Papers in Press, January 20, 2012, DOI 10.1074/jbc.M111.308601

Jessica L. Wittnam[‡], Erik Portelius[§], Henrik Zetterberg[§], Mikael K. Gustavsson[§], Stephan Schilling[¶], Birgit Koch[¶], Hans-Ulrich Demuth[¶], Kaj Blennow[§], Oliver Wirths[‡], and Thomas A. Bayer[‡1]

From the [‡]Division of Molecular Psychiatry, Georg August University Göttingen, University Medicine Göttingen, 37075 Göttingen, Germany, the [§]Clinical Neurochemistry Laboratory, Department of Psychiatry and Neurochemistry, Institute of Neuroscience and Physiology, The Sahlgrenska Academy, University of Gothenburg, 413 45 Mölndal, Sweden, and [¶]Probiodrug AG, 06120 Halle (Saale), Germany

Background: Pyroglutamate Aβ is an abundant, toxic peptide in Alzheimer disease brain.
Results: Pyroglutamate Aβ aggravates the pre-existing behavioral phenotype of 5XFAD mice.
Conclusion: These results support a major pathological function of pyroglutamate Aβ in Alzheimer disease.
Significance: The data further indicate that pyroglutamate Aβ is an important therapeutic target.

Pyroglutamate-modified Aβ peptides at amino acid position three ($Aβ_{pE3-42}$) are gaining considerable attention as potential key players in the pathogenesis of Alzheimer disease (AD). $Aβ_{pE3-42}$ is abundant in AD brain and has a high aggregation propensity, stability and cellular toxicity. The aim of the present work was to study the direct effect of elevated $Aβ_{pE3-42}$ levels on ongoing AD pathology using transgenic mouse models. To this end, we generated a novel mouse model (TBA42) that produces $Aβ_{pE3-42}$. TBA42 mice showed age-dependent behavioral deficits and $Aβ_{pE3-42}$ accumulation. The Aβ profile of an established AD mouse model, 5XFAD, was characterized using immunoprecipitation followed by mass spectrometry. Brains from 5XFAD mice demonstrated a heterogeneous mixture of full-length, N-terminal truncated, and modified Aβ peptides: $Aβ_{1-42}$, $Aβ_{1-40}$, $Aβ_{pE3-40}$, $Aβ_{pE3-42}$, $Aβ_{3-42}$, $Aβ_{4-42}$, and $Aβ_{5-42}$. 5XFAD and TBA42 mice were then crossed to generate transgenic FAD42 mice. At 6 months of age, FAD42 mice showed an aggravated behavioral phenotype compared with single transgenic 5XFAD or TBA42 mice. ELISA and plaque load measurements revealed that $Aβ_{pE3}$ levels were elevated in FAD42 mice. No change in $Aβ_{x-42}$ or other Aβ isoforms was discovered by ELISA and mass spectrometry. These observations argue for a seeding effect of $Aβ_{pE-42}$ in FAD42 mice.

Alzheimer disease (AD)[2] is a progressive neurodegenerative disorder characterized by the presence of extracellular amyloid plaques composed of amyloid-β (Aβ) and intracellular neurofibrillary tangles. The discovery that certain early onset familial forms of AD may be caused by enhanced levels of Aβ peptides led to the hypothesis that amyloidogenic Aβ is intimately involved in the pathogenic process (1).

Analysis of amyloid deposits in AD brains revealed various N- and C-terminal variants (2–4). The increased C-terminal length of Aβ (from $Aβ_{x-40}$ to $Aβ_{x-42}$) in AD enhances its aggregation properties. Faster aggregation leads to earlier Aβ deposition, which is believed to promote its toxicity (5–7). Recently, $Aβ_{1-43}$ was discovered as a novel toxic peptide in AD (8, 9). In addition to Aβ peptides starting with aspartate as the first amino acid ($Aβ_1$), several N-terminal truncated and modified Aβ species have also been described. These Aβ isoforms include a truncated peptide starting at position 4, first reported in 1985 by Masters *et al.* (2, 10–12). Mass spectrometric analysis of AD brain tissue showed that an N-terminal truncated isoform of Aβ starting with pyroglutamate ($Aβ_{pE3}$) is frequently present, thus explaining, at least partially, the initial difficulties in sequencing Aβ peptides purified from human brain tissue (16). Later immunohistochemical studies of human brain identified $Aβ_{pE3}$ as a major component of Aβ plaques (12, 13). More recently, immunoprecipitation in combination with mass spectrometry confirmed $Aβ_{pE3-42}$ as a dominant Aβ isoform in the hippocampus and cortex of AD patients (14, 15).

Saido *et al.* (12) suggested that removal of N-terminal amino acids 1 and 2 of Aβ might be carried out by a hypothetical amino or dipeptidyl peptidase(s), followed by a putative glutamate cyclization activity. Also, aminopeptidase A may be

[S] This article contains supplemental "Experimental Procedures," Table 1, Figs. 1–3, and additional references.

[1] To whom correspondence should be addressed: Div. of Molecular Psychiatry, Georg-August-University Göttingen, University Medicine Göttingen, Von-Siebold-Strasse 5, 37075 Göttingen, Germany. E-mail: tbayer@gwdg.de.

[2] The abbreviations used are: AD, Alzheimer disease; Aβ, amyloid β; $Aβ_{1-40}$, full-length $Aβ_{1-40}$; $Aβ_{1-42}$, full-length $Aβ_{1-42}$; $Aβ_{x-40}$, N-terminal truncated Aβ40 with an unspecified N terminus; $Aβ_{x-42}$, N-terminal truncated $Aβ_{42}$ with an unspecified N terminus; $Aβ_{1-x}$, Aβ starting with amino acid one with an unspecified C terminus; $Aβ_{3-x}$, Aβ starting with amino acid three with an unspecified C terminus; $Aβ_{Q3-42}$, $Aβ_{42}$ starting with glutamine at the third amino acid position; $Aβ_{pE3}$, pyroglutamate Aβ beginning at the third amino acid position; $Aβ_{pE3-42}$, $Aβ_{42}$ with an N-terminal pyroglutamate modification beginning at the third amino acid position; $Aβ_{pE3-x}$, pyroglutamate Aβ beginning at the third amino acid position with an unspecified C terminus; $Aβ_{4-42}$, N-terminal truncated Aβ starting with amino acid four and ending with amino acid 42; $Aβ_{5-42}$, N-terminal truncated Aβ starting with amino acid five and ending with amino acid 42; APP, amyloid precursor protein; EPM, elevated plus maze; FA, formic acid; hQC, human glutaminyl cyclase; IP, immunoprecipitation; ANOVA, analysis of variance.

responsible in part for the N-terminal truncation of full-length Aβ peptides (16). The enzyme glutaminyl cyclase (QC) was later identified and discovered to also catalyze not only glutamine but is responsible for N-terminal glutamate conversion generating $A\beta_{pE3}$ or $A\beta_{pE11}$ from their glutamate precursors (17, 18).

Experiments involving various mouse models have highlighted the toxicity of $A\beta_{pE3}$. Overexpression of $A\beta_{pE3-42}$ in the brains of transgenic mice triggers neuron loss and an associated neurological phenotype (19, 20). Blocking QC function, either through genetic knock-out (21) or pharmacological inhibition (22), lowers $A\beta_{pE3}$ levels, decreases plaque load, and ameliorates behavioral deficits in different AD mouse models. Conversely, crossing 5XFAD mice with transgenic mice expressing human QC (hQC) significantly increases levels of soluble $A\beta_{pE3-42}$ peptides, raises plaque load, and intensifies motor and working memory impairment (21).

The aim of the present study was to investigate how additional $A\beta_{pE3-42}$ impacts the progression of AD pathology independent of QC manipulations. To accomplish this, we crossed a novel transgenic mouse model that produces $A\beta_{pE3-42}$ (TBA42) to an established AD mouse model (5XFAD). The 5XFAD mouse model expresses mutant human APP695 (Swedish, Florida, and London mutations) together with presenilin-1 (PS1) containing the M146L and L286V mutations. 5XFAD mice develop age-dependent behavioral deficits, axonopathy, neuron loss, and robust plaque pathology (23, 24). We then analyzed the effects of elevated $A\beta_{pE3-42}$ on the behavioral phenotype, co-precipitation of other Aβ variants, and plaque load pathology in the resulting transgenic mice (FAD42). Our findings demonstrate that an increase in $A\beta_{pE3-42}$ can adversely affect the strong and robust AD phenotype of 5XFAD mice.

EXPERIMENTAL PROCEDURES

Transgenic Mice—The generation of the transgenic vector expressing murine thyrotropin-releasing hormone-Aβ (mTRH-$A\beta_{3-42}$) under the control of the murine Thy1.2 regulatory sequence was described previously (17, 19, 20). The glutamate at position three of the Aβ amino acid sequence was mutated into glutamine to facilitate enhanced pyroglutamate formation. The mice thus express unmodified $A\beta_{3Q-42}$ (designated as $A\beta_{3-42}$), which can be readily converted to $A\beta_{pE3-42}$ by QC. TBA42 mice were generated by male pronuclear injection of fertilized C57BL/6J oocytes. The resulting offspring were screened for transgene integration by PCR analysis. Three founder animals (TBA41, TBA42, and TBA45) were identified and subsequently bred to C57BL/6J mice to establish independent lines. Transgene expression was assessed in the F1 generation of each line using RT-PCR. The line with the highest transgene mRNA expression was selected for further breeding (named truncated beta-amyloid 42; TBA42).

5XFAD mice were described previously (23). The APP695 and PS1 transgenes co-segregate and are both under the control of the murine Thy1.2 regulatory sequence. All 5XFAD mice were back-crossed for >10 generations onto a C57BL/6J genetic background.

FAD42 mice were generated by breeding transgene positive 5XFAD mice to transgene positive TBA42 mice. Wild-type, transgenic offspring were identified subsequently using PCR. All animal experiments were conducted in accordance with the German guidelines for animal care and approved by the local legal authorities. Only female mice were used in this study.

Behavioral Tests—Mice were group-housed with an average of four individuals per cage and kept on a 12 h/12 h inverted light cycle (lights off at 8:00 AM). Free access to food and water was provided. Behavioral testing was performed during the dark phase under red lighting.

The balance beam, cross-maze, and elevated plus maze (EPM) were performed as described previously (24, 25). For the cross-maze, spontaneous alternation rates were calculated as the percentage of actual alternations made relative to the total number of possible alternations.

Anxiety was measured in the EPM by determining the percentage of time spent in the open arms of the apparatus during a 5-min period. All EPM data were collected using the ANY-maze video tracking system (Stoelting, Wood Dale, IL).

Immunohistochemistry—Mouse tissue was processed as described previously (26). In brief, 4-μm paraffin sections were deparaffinized in xylene and rehydrated in a series of ethanol baths. Sections were pretreated with 0.3% H_2O_2 in PBS to block endogenous peroxidases. Antigen retrieval was achieved by boiling sections in 0.01 M citrate buffer (pH 6.0), followed by a 3-min incubation in 88% formic acid (FA). Nonspecific antigens were blocked using a solution of 10% FCS and 4% skim milk powder in PBS. Sections were incubated in primary antibody solution overnight at room temperature, washed, and then incubated for 1 h with biotinylated secondary antibody solution. Staining was visualized using the Vectastain kit (Vector Laboratories, Burlingame, CA) and 3,3′-diaminobenzidine (Sigma-Aldrich). Microscopy was performed on an Olympus BX-51 microscope equipped with a DP-50 camera (Olympus, Hamburg, Germany).

Antibodies—The following anti-Aβ antibodies were used for immunohistochemistry and immunoprecipitation (IP), as indicated: 4G8 (Aβ epitope 17–24; Covance, Princeton, NJ), 6E10 (Aβ epitope 4–9; Signet Laboratories, Inc., Dedham, MA), G2–11 (Aβ epitope at the C terminus of Aβ42 (27)), Aβ[N] (IBL America, Minneapolis, MN), 1–57 and 2–48 (both against N-terminal $A\beta_{pE3}$ (26), Synaptic Systems, Göttingen, Germany). Glial fibrillary acidic protein (mouse monoclonal, Synaptic Systems) was used for immunohistochemistry. Biotinylated goat anti-mouse and swine anti-rabbit immunoglobulins (DAKO, Glostrup, Denmark) were used as secondary antibodies for immunohistochemistry.

Mass Spectrometric Analysis—Homogenization of brain tissue was performed as described previously (28). Briefly, the brains (~50 mg) were homogenized (Pellet Pestle®, Sigma-Aldrich®) on ice in TBS (20 mM Tris, 137 mM NaCl, pH 7.6) with complete protease inhibitor tablets (Roche Applied Science, Basel, Switzerland). The extraction ratio (brain tissue:TBS) was 1:5 (weight/volume). FA was added to the sample (final concentration, 70%) followed by sonication (power, 15; Amplit.microns; TUne, "middle") and centrifugation at 30,000 × *g* for 1 h at 4 °C. The FA-soluble Aβ extract was dried and dissolved in FA and finally neutralized using 0.5 M Tris.

IP using the KingFisher magnetic particle processor (Thermo Scientific) and mass spectrometric analysis using MALDI TOF/TOF MS were performed as described previously (29). Briefly, an aliquot (4 μl, 1 mg/ml) of the Aβ-specific antibodies 6E10 and 4G8 was separately added to 50 μl of Dynabeads M-280 sheep anti-mouse IgG (Invitrogen) according to the manufacturer's instructions. The washed beads with bound antibody (50 μl of 6E10 and 50 μl of 4G8) were combined and used for IP of the neutralized FA fraction. IP of brain tissue with the antibody 1–57 was conducted as described above.

The beads/FA fraction was transferred to a KingFisher magnetic particle processor for automatic washing and elution of the Aβ isoforms. The collected supernatant was dried in a vacuum centrifuge and redissolved in 5 μl of 0.1% FA in 20% acetonitrile. MS measurements were performed using a Bruker Daltonics UltraFlex MALDI TOF/TOF instrument (Bruker Daltonics, Bremen, Germany).

ELISA of Aβ Levels in Brain—Mice were sacrificed using cervical dislocation. Brains were dissected rapidly on ice, the olfactory bulb and cerebellum were removed, and the hemispheres were separated. Brains were frozen on dry ice and stored at −80 °C until use. Frozen brains (n = 3–4 per group) were homogenized on ice in TBS (120 mM NaCl, 50 mM Tris, pH 8.0) containing complete protease inhibitor tablets (Roche Applied Science)) using a Dounce homogenizer. The extraction ratio (brain tissue:TBS) was 1:8 (weight/volume). Samples were centrifuged at 27,000 × g for 20 min at 4 °C. Supernatants (TBS fractions) were removed, and the remaining pellets were resuspended in 0.8 ml of 2% SDS with complete protease inhibitor, sonicated, and centrifuged at 27,000 × g for 15 min at 4 °C. The resulting supernatants (SDS fractions) were treated with 1 μl of Benzonase (Novagen, Darmstadt, Germany) and incubated for 10 min at 4 °C on rotary wheel. All fractions were stored at −80 °C until use. ELISA measurements of $Aβ_{x-42}$ and $Aβ_{pE3}$ in the TBS and SDS fractions were performed in triplicate according to the manufacturer's instructions (IBL Intl., Hamburg, Germany). Aβ levels were normalized to brain wet weight.

Quantification of Plaque Load—Extracellular Aβ plaque load was calculated from serial images of the cortex (100× magnification) taken from sagittal sections spaced a minimum of 20 μm apart. Four sections were evaluated per animal (n = 5–7 per group). Using NIH ImageJ software (version 1.41), images were converted into an eight-bit black-and-white format. Image thresholds were set to a fixed value to define the total plaque area. Thresholds were selected to maximize the plaque area detected while minimizing the contribution of intracellular Aβ accumulations. Plaque load was calculated as the percentage area occupied by Aβ immunostaining.

Statistical Analysis—Statistical differences were evaluated using one-way or two-way analysis of variance (ANOVA) followed by Bonferroni post hoc tests or unpaired t test, as indicated. All data are given as means ± S.E. All statistics were calculated using GraphPad Prism (version 5.0, GraphPad Software, San Diego, CA).

RESULTS

Generation and Characterization of TBA42 Mice—To study the role of $Aβ_{pE3-42}$ in AD more precisely, we generated the TBA42 transgenic mouse model. The TBA42 transgene was designed to preferentially liberate $Aβ_{3-42}$ peptides into the neuronal secretory pathway. This allows QC to enzymatically catalyze the conversion of $Aβ_{3-42}$ to $Aβ_{pE3-42}$ (16, 17, 21).

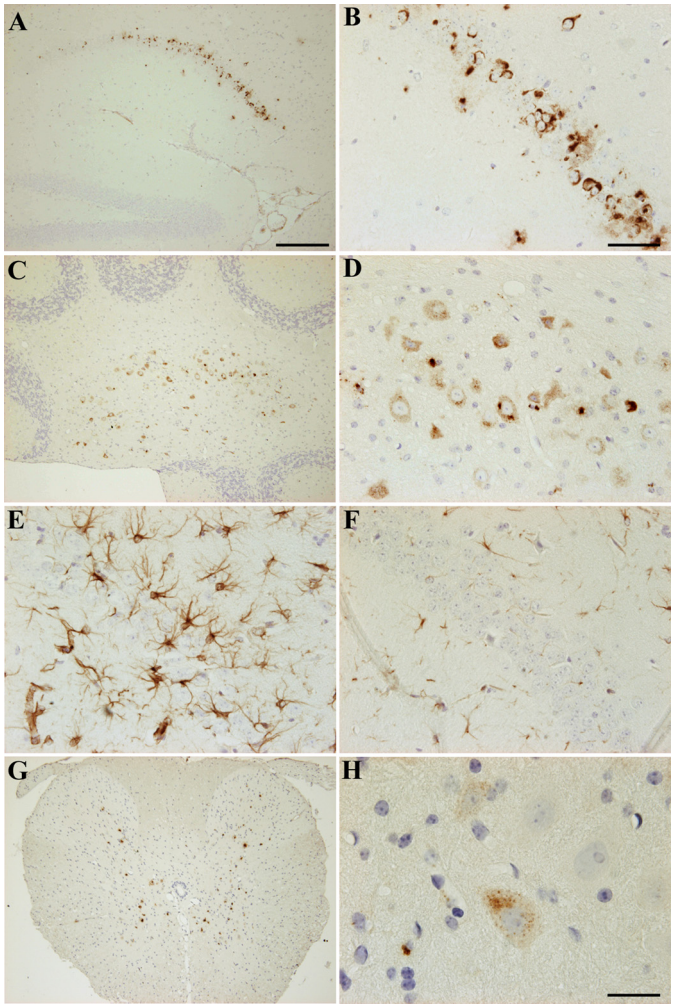

FIGURE 1. **Aβ accumulation and gliosis in TBA42 mice.** TBA42 mice accumulated abundant intraneuronal Aβ in CA1 pyramidal neurons of the hippocampus by 3 months of age (*A* and *B*). 6-month-old TBA42 mice showed marked intraneuronal Aβ accumulation in cerebellar nuclei (*C* and *D*). Strong astrogliosis, a marker for neurodegeneration, was present in the CA1 region of the hippocampus in 12-month-old TBA42 mice (*E*) and absent in age-matched control mice (*F*). 12-month-old TBA42 mice demonstrated Aβ accumulation in the spinal cord (*G* and *H*). Note the example of prominent intraneuronal Aβ in *H*. *Scale bars*, *A*, *C*, and *G* = 200 μm; *B*, *D*, *E*, and *F* = 50 μm; *H* = 20 μm.

Transgene expression was assessed in TBA42 mice using immunohistochemistry. Intraneuronal accumulation of Aβ peptides was observed in the hippocampus by the age of 3 months (Fig. 1, *A* and *B*). At 6 months of age, intraneuronal Aβ was also seen in cerebellar nuclei (Fig. 1, *C* and *D*). Interestingly, analysis of 12-month-old TBA42 mice revealed marked gliosis in the hippocampus (Fig. 1, *E* and *F*) and additional Aβ in spinal cord motor neurons (Fig. 1, *G* and *H*). Signs of gliosis, an indicator of ongoing neurodegeneration, were absent in age-matched WT mice (Fig. 1, *E* and *F*). This finding suggests that gliosis is a consequence of the Aβ aggregation in TBA42 mice. Extracellular Aβ deposits were rarely detected in TBA42 mice at all of the ages analyzed.

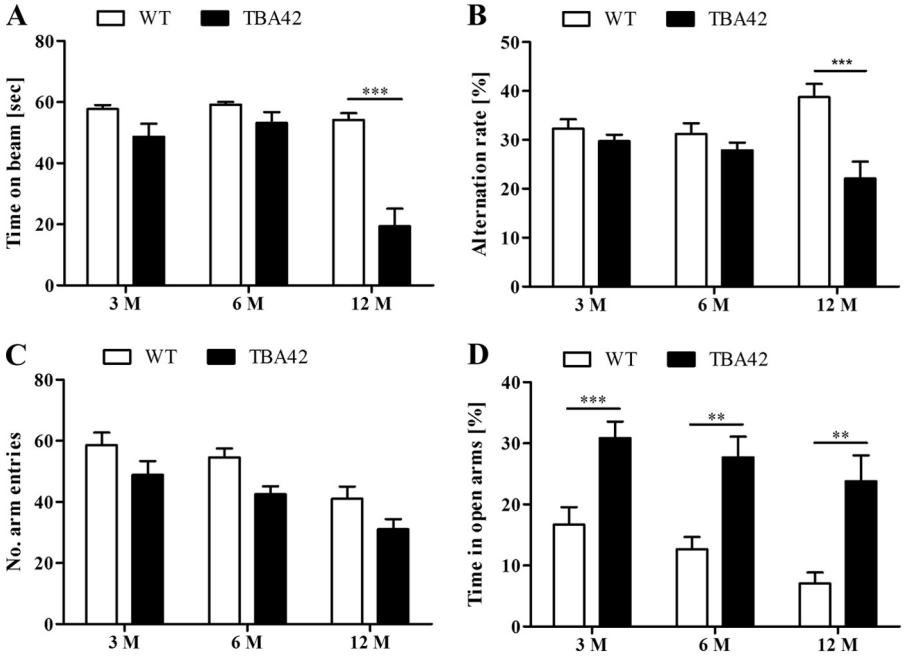

FIGURE 2. **Alterations in age-dependent motor function, working memory, and anxiety in TBA42 mice.** The behavioral phenotype of TBA42 mice was assessed at 3, 6, and 12 months (*M*) of age. TBA42 mice demonstrated significantly reduced performance in the balance beam (*A*) and the cross-maze tasks (*B*) at the age of 12 months. There was no difference in the number of arm entries in the cross-maze task between TBA42 and wild-type control (*C*). The elevated plus maze revealed that TBA42 mice already had highly reduced anxiety levels by the age of 3 months (*D*) (two-way ANOVA with Bonferroni post hoc tests; *, $p < 0.05$; **, $p < 0.01$; ***, $p < 0.001$; $n = 6$–12 per group).

Behavioral Analysis of TBA42 Mice—To determine whether functional impairments accompanied the observed brain pathology, we subjected cohorts of 3-, 6-, and 12-month-old TBA42 mice to a battery of behavioral tests. The balance beam was selected to evaluate general motor coordination. Three and 6-month-old mice performed comparably wtih WT animals. However, by the age of 12 months, TBA42 mice showed significant impairment ($p < 0.001$; Fig. 2*A*). Similarly, assessment of working memory in the cross-maze demonstrated that only 12-month-old TBA42 mice had noticeable deficits in this task ($p < 0.001$; Fig. 2*B*).

AD mouse models can show decreases in anxiety in addition to memory deficits (24, 30), and changes in anxiety are commonly detected using the EPM. In this task, animals with lower anxiety levels spend greater amounts of time on the open arms of the apparatus and less time in the closed arms. When TBA42 mice were tested in the EPM, a striking decrease in anxiety was already observed in 3-month-old mice ($p < 0.001$). This reduction persisted at the later time points tested ($p < 0.01$; Fig. 2*C*). Taken together, these data demonstrate that the Aβ accumulation in theTBA42 mice is sufficient to induce age-dependent behavioral deficits.

To study the potential effect of elevated $A\beta_{pE3-42}$ in a conventional AD mouse model, we crossed TBA42 with 5XFAD mice. Extracellular plaque pathology is present by 3 months of age in 5XFAD mice, and age-dependent behavioral deficits are first observed in 6-month-old animals (23, 24).The resulting transgenic mice (termed FAD42) were investigated using mass spectrometry, behavioral tests, ELISA, and plaque load analysis.

Immunoprecipitation and Mass Spectrometric Characterization of Wild-type, TBA42, 5XFAD, and FAD42 Mouse Brain—Using the two antibodies 6E10 and 4G8 in the IP experiments, a distinct Aβ isoform pattern consisting of $A\beta_{5-42}$, $A\beta_{4-42}$, $A\beta_{1-40}$, and $A\beta_{1-42}$ was detected in the FA-extracted brain tissues from 5XFAD mice (Fig. 3, for representative mass spectra). The most dominant form was the peak representing $A\beta_{1-42}$. A similar pattern was detected in the transgenic model FAD42. TBA42 mice displayed no peaks corresponding to Aβ using 6E10 and 4G8. However, using the N-terminal-specific Aβ antibody 1–57, $A\beta_{pE3-42}$ and unmodified $A\beta_{3-42}$ were detected in TBA42, 5XFAD, and in FAD42 mice whereas $A\beta_{pE3-40}$ was only detected in 5XFAD mice. Interestingly, no major difference in the pattern of different Aβ variants isolated after IP was found between 6-month-old 5XFAD and FAD42 mice. In all cases unmodified $A\beta_{3-42}$ was much less abundant than $A\beta_{pE3-42}$. No peaks corresponding to Aβ were detected in WT mice using either the 4G8 and 6E10 or the 1–57 antibodies. These results confirm that 5XFAD mice harbor a heterogeneity of N-terminal truncated and modified Aβ peptides, but TBA42 mice express only $A\beta_{pE3-42}$ and unmodified $A\beta_{3-42}$. Interestingly, no gross difference in the pattern of different Aβ variants isolated after IP was found between 6-month-old 5XFAD and FAD42 mice. A minor peak of $A\beta_{pE3-40}$ was detected in 5XFAD mice and not in the other models investigated. Although the Aβ isoforms detected in the mass spectrum cannot be interpreted as a direct reflection of their abundance in the brain because the ionization efficiency can vary for the different isoforms, we cannot completely rule out a significant precipitation of $A\beta_{pE3-40}$ in 5XFAD alone. It could be that the loss of the weak $A\beta_{pE3-40}$ signal is likely due to differential ionization efficiency not reflecting a true precipitation difference between 5XFAD and FAD42 mice. Moreover, it cannot be excluded that the different levels of $A\beta_{pE3}$ variants between 5XFAD and FAD42 mice are due to highly aggregated $A\beta_{pE3}$ in the FAD42 animals and may have therefore been not efficiently extracted for IP-MS analysis.

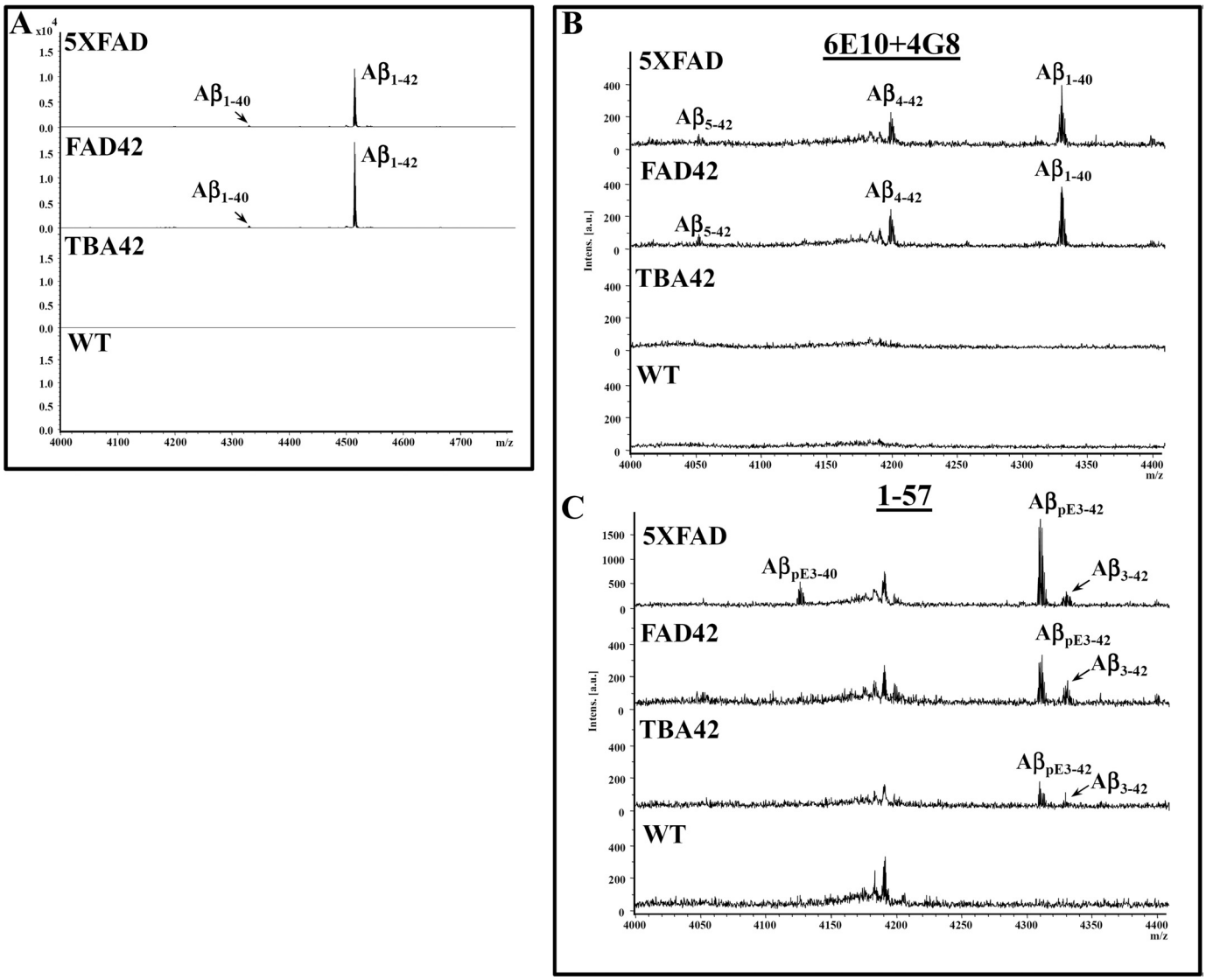

FIGURE 3. **N-terminal heterogeneity of Aβ peptides in 5XFAD and FAD42 mice.** Mass spectra of immunoprecipitated Aβ peptides from the brains of mice using pan-Aβ antibodies 6E10 and 4G8 (*A* and *B*; used as a mix) and the N-terminal-specific antibody 1–57 (*C*) recognizing both pyroglutamate $A\beta_{pE3}$ and unmodified $A\beta_3$ peptides. *A*, the dominant fraction in 5XFAD and FAD42 mice was $A\beta_{1-42}$, followed by $A\beta_{1-40}$, $A\beta_{pE3-42}$, $A\beta_{4-42}$, $A\beta_{pE3-40}$, and $A\beta_{3-42}$. *B*, there was no significant difference in the pattern between 5XFAD and FAD42 mice. *C*, using 1–57 for IP-MS, N-terminal truncated $A\beta_{pE-42}$ was the major peptide detected in 5XFAD, FAD42, and TBA42. No Aβ was detected in WT mice.

Behavioral Analysis of FAD42 Mice—To evaluate the effects of additional $A\beta_{pE3-42}$ on the behavioral phenotype of 5XFAD mice, we tested 6-month-old WT, 5XFAD, TBA42, and FAD42 mice in the balance beam and EPM. Motor performance was significantly impaired in the FAD42 mice as shown by the balance beam ($p < 0.001$; Fig. 4*A*). In addition, the EPM revealed that anxiety levels were even further decreased in FAD42 mice ($p < 0.001$; Fig. 4*B*). These data indicate that the extra $A\beta_{pE3-42}$ resulting from the TBA42 transgene in the FAD42 mice is sufficient to enhance the behavioral deficits observed in 5XFAD single transgenic mice.

Aβ Accumulation in FAD42 Mice—To assess the impact of additional $A\beta_{pE3-42}$ on total Aβ deposition, cortical plaque load was measured in 6-month-old 5XFAD and FAD42 mice. A significant increase in the ratio of $A\beta_{pE3}$ to $A\beta_{1-x}$ plaque area was observed between 5XFAD and FAD42 mice (5XFAD, 0.93 ± 0.1; FAD42, 1.5 ± 0.12; Fig. 5, *A–D* and *G*). The ratio of $A\beta_{x-42}$ to $A\beta_{1-x}$ plaque area remained unchanged (5XFAD, 1.7 ± 0.23; FAD42, 2.56 ± 0.52; Fig. 5, *C–G*). These findings indicate that the additional $A\beta_{pE3-42}$ in FAD42 mice enhances seeding and increases plaque deposition relative to 5XFAD mice. No obvious changes in the intraneuronal Aβ pattern were detected between 5XFAD and FAD42 mice in the primary motor cortex (supplemental Fig. S1). The observation of increased plaque load and increased pyroglutamate Aβ pools using ELISA in FAD42 mice argues for a major contribution of extracellular soluble Aβ pools. Interestingly, in the spinal cord, hippocampus and cerebellum, we did see an apparent increase in the number of neurons with intracellular Aβ in FAD42 compared with TBA42 and 5XFAD (supplemental Fig. S2).

Frozen brains from 6-month-old 5XFAD, TBA42 and FAD42 mice were subjected to sequential protein extractions in TBS- and SDS-based buffers. ELISA was then used to measure

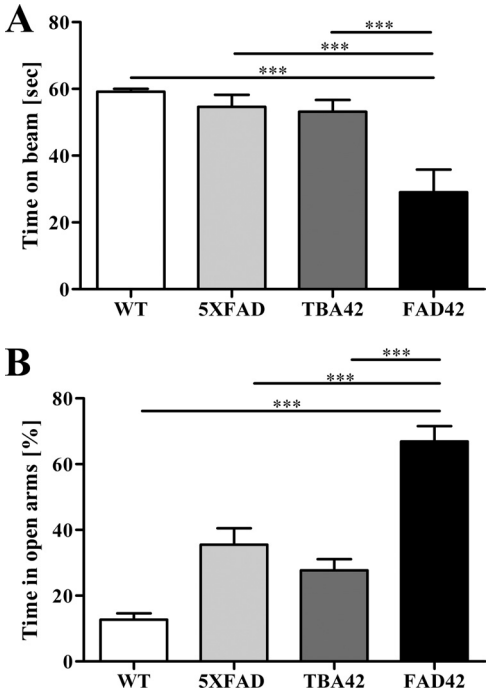

FIGURE 4. **Aggravated behavioral impairments in FAD42 mice.** Motor function and anxiety were assessed in 6-month-old WT, 5XFAD, TBA42, and FAD42 mice using the balance beam (*A*) and elevated plus maze (*B*), respectively. In both tasks, transgenic FAD42 mice showed increased impairment relative to the WT and single transgenic 5XFAD and TBA42 animals (one-way ANOVA with Bonferroni post hoc tests). ***, $p < 0.001$ ($n = 5–9$ per group).

levels of soluble (TBS) and insoluble (SDS) $A\beta_{x-42}$ and $A\beta_{pE3-x}$ (mass Aβ/g brain). Levels of TBS-soluble $A\beta_{x-42}$ were significantly higher in the 5XFAD (162.8 ± 22.2 (ng/g)) and FAD42 mice (154.7 ± 13.8 (ng/g)) than in TBA42 mice (8.2 ± 0.4 (ng/g), $p < 0.001$; Fig. 6*A*). Similarly, in the SDS fraction, 5XFAD (32,032 ± 13,803 (ng/g)) and FAD42 mice (31,771 ± 14,234 (ng/g)) had more $A\beta_{x-42}$ than TBA42 mice (11 ± 0.5 (ng/g)) (Fig. 6*C*). TBS-soluble $A\beta_{pE3-x}$ levels were substantially higher in FAD42 mice (238.4 ± 67.8 pg/g) than in TBA42 mice (51.25 ± 7.5 pg/g; $p < 0.05$) and elevated relative to 5XFAD mice (141 ± 28.5 pg/g) (Fig. 6*B*). Notably, the amount of SDS-soluble $A\beta_{pE3-x}$ was significantly higher in the FAD42 mice (29,061 ± 2,805 pg/g) in comparison with both the TBA42 (3,714 ± 485 pg/g; $p < 0.001$) and 5XFAD mice (15,826 ± 1,547 pg/g; $p < 0.01$). Significant differences in the levels of SDS-soluble $A\beta_{pE3-x}$ were also observed between TBA42 and 5XFAD mice ($p < 0.01$; Fig. 6*D*). Compared with other transgenic mouse models and AD patients, the TBA42 model produces medium levels of $A\beta_{pE3}$. Interestingly, the FAD42 mouse line has comparable levels as observed in the brain of AD patients with Braak stage I and II (supplemental Table 1). The observed up-regulated QC activity was not unexpected because Schilling *et al.* (22) have shown massive increase of QC mRNA and higher QC activity in AD brain samples previously (supplemental Fig. 3). QC is found in astrocytes making plausible that QC activity could change in response to the Aβ pathology in AD (1). The physiological background of this phenotype is presently under intense investigation.

DISCUSSION

The aim of the current report was to study the direct effect of an $A\beta_{pE3-42}$ increase in 5XFAD mice, a conventional AD mouse model expressing human mutant APP and PS1 transgenes. We could demonstrate that $A\beta_{pE3-42}$ induces age-dependent behavioral deficits in TBA42 mice. This finding is consistent with previous studies in similar transgenic models expressing $A\beta_{pE3-42}$ (19, 20). Transgenic expression of hQC in 5XFAD mice also leads to the elevation of $A\beta_{pE3}$, thereby exacerbating behavioral deficits, increasing plaque load, and raising levels of $A\beta_{pE3-42}$ but not general $A\beta_{x-42}$. It should be noted that QC has several targets besides $A\beta_{3-x}$, and these substrates could potentially influence the phenotype of the transgenic 5XFAD/hQC mice in the previous study (21). N-terminal pyroglutamate residues have been described for a number of hormones and secreted proteins (31). For example, the N terminus of monocyte chemoattractant protein 1 (CCL2/MCP-1) is modified to a pyroglutamate residue, thereby protecting it against degradation (32). MCP-1 plays a pivotal role in different inflammatory conditions (33). As microglial activity could contribute to neuron dysfunction (33), a potential effect of QC overexpression on microglia-mediated inflammation in transgenic 5XFAD/hQC mice cannot be ruled out.

Using mass spectrometric analysis, we demonstrated that 5XFAD mice already exhibit high amounts of $A\beta_{pE3-42}$ and other Aβ isoforms. Our findings corroborate earlier works identifying $A\beta_{1-42}$ as the dominant Aβ peptide present in the brains of 5XFAD mice (21, 23, 24). Besides $A\beta_{1-42}$, the following peptides were detected in 5XFAD mice, in order of abundance: $A\beta_{1-40}$, $A\beta_{4-42}$, $A\beta_{5-42}$, $A\beta_{pE3-42}$, and $A\beta_{3-42}$. The appearance of an exceedingly heterogeneous population of N-terminal truncated and modified Aβ peptides in 5XFAD mice is in line with previous observations made in the APP/PS1KI mouse model (34).

Levels of N-terminal truncated and modified Aβ are known to vary between AD mouse models. In Tg2576 mice, truncated and modified Aβ isoforms do not appear before 1 year of age and comprise ~5% of total Aβ (35). $A\beta_{pE3}$ and other modified forms of Aβ were reported to be absent in APP23 mice until almost 2 years of age (36) or low in PS2APP mice (15). Using another approach, Maeda and colleagues (37) demonstrated that the localization and abundance of [^{11}C]PIB autoradiographic signals were associated closely with $A\beta_{pE3}$ plaques in AD and different APP transgenic mouse brains. This observation suggests that the [^{11}C]PIB-PET retention signal depends on the accumulation of specific Aβ subtypes (37). Interestingly, significant brain area-specific neuron loss develops in both APP/PS1KI and 5XFAD mice (23, 24, 34, 38–40). In other AD mouse models, neuron loss is much less prevalent (41). Taken together, these findings suggest that truncated and modified Aβ peptides have an important implication for neurodegeneration in murine models of AD.

The TBA42 mouse model, like the previously published TBA2, TBA2.1, and TBA2.2 models (19, 20), expresses $A\beta_{3Q-42}$ starting with an N-terminal glutamine (Gln) residue at position three of Aβ. Glutamine was used instead of the naturally occurring glutamate because it is a better substrate for

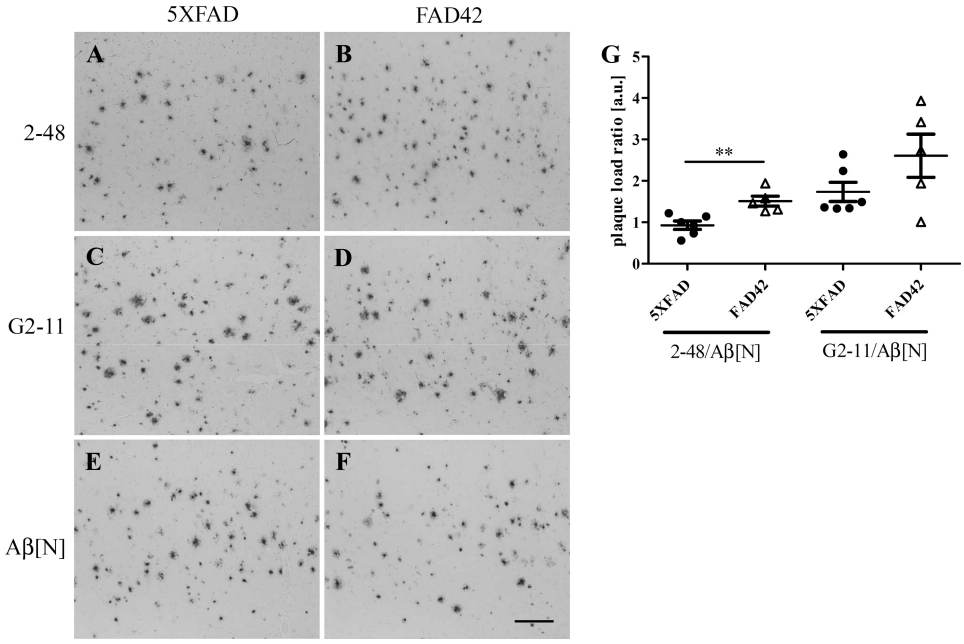

FIGURE 5. **Elevated plaque pathology in the cortex of FAD42 mice.** Immunostaining with pyroglutamate-Aβ-specific antibody 2–48 in 5XFAD (*A*) and FAD42 (*B*) mice, with C-terminal specific antibody G2–11 against Aβ_{x-42} in 5XFAD (*C*) and FAD42 (*D*) mice, and Aβ_{1-x} specific antibody Aβ[N] in 5XFAD (*E*) and FAD42 (*F*) mice. There was a significant difference in the plaque load expressed as a ratio of antibody 2–48 *versus* antibody Aβ[N] between 5XFAD and transgenic FAD42 mice (*G*). No difference was found in the ratio of G2–11 *versus* Aβ[N]. One-way ANOVA and unpaired *t* test; **, $p < 0.01$. *a.u.*, arbitrary units. *Scale bar*, 200 μm.

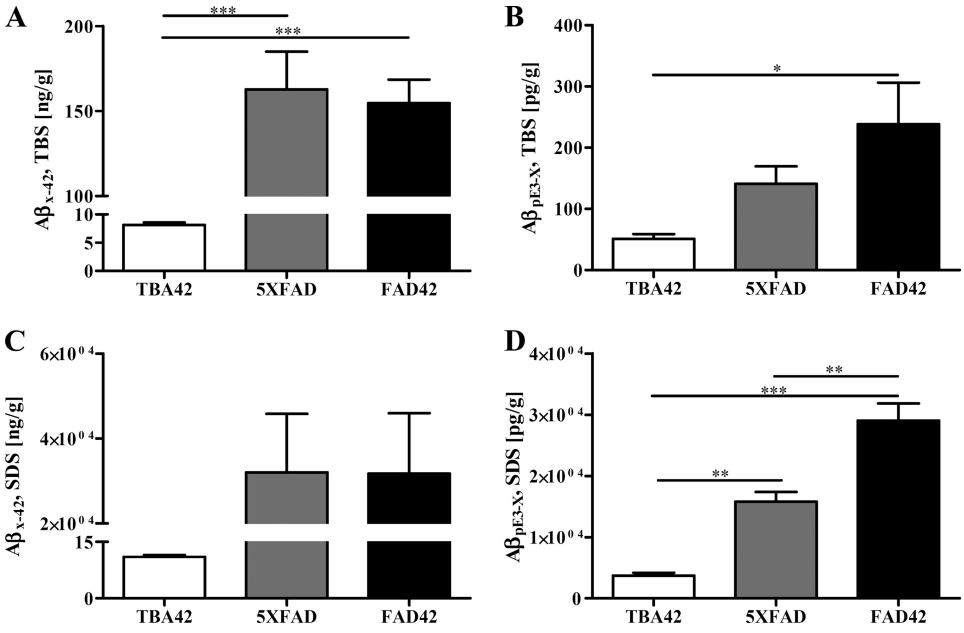

FIGURE 6. **Increased levels of Aβ_{pE3} in the brains of FAD42 mice as shown by ELISA.** 5XFAD and FAD42 mice demonstrated elevated Aβ_{x-42} levels in the TBS- (*A*) and SDS-soluble (*C*) fraction compared with TBA42 mice. There was no significant difference between the Aβ_{x-42} levels in 5XFAD and FAD42 mice for either fraction. In all mouse lines, the SDS soluble fraction of Aβ_{x-42} harbored the most Aβ peptides. The levels of TBS-soluble Aβ_{pE3-x} were significantly higher in FAD42 mice compared with TBA42 mice (*B*). Substantially more SDS-soluble Aβ_{pE3-x} was detected in FAD42 mice relative to both 5XFAD and TBA42 mice (*D*) (one-way ANOVA and unpaired *t* tests). *, $p < 0.05$; **, $p < 0.01$; ***, $p < 0.001$.

both the spontaneous and enzymatically catalyzed conversion of Aβ_{3-42} into Aβ_{pE3-42} (17). The degree of conversion was not determined in the TBA2, TBA2.1, and TBA2.2 mice. Therefore, unmodified N-terminal truncated Aβ_{3-42} could also contribute to the observed pathology and behavioral phenotype. Mass spectrometric analysis revealed that the majority of Aβ in the TBA42 mice was indeed pyroglutamated, and only a minor portion was left unmodified. However, it cannot be excluded that the unmodified Aβ_{3-42} also participates in the observed deficits. It should be noted that passive immunization against low molecular weight pyrogutamate-modified Aβ oligomers produces beneficial therapeutic effects in 5XFAD mice (39). These data imply that a change in the amount of Aβ_{pE3} is sufficient to affect pathology despite the presence of other Aβ isotypes.

Analysis of water soluble Aβ in AD, Down syndrome, and non-demented elderly brain specimens indicated the presence

of $A\beta_{1-42}$, $A\beta_{pE3-42}$, and $A\beta_{pE11-42}$ (42). AD cases with PS1 mutations develop a higher ratio of water-soluble $A\beta_{pE3-42}$ and$A\beta_{pE11-42}$ to full-length $A\beta_{1-42}$ in comparison with sporadic AD cases (43). Overall, the ratio of water-soluble $A\beta_{pE3-42}$ to $A\beta_{1-42}$ seems to be proportional to the clinical phenotype and the severity of AD and DS. Kuo *et al.* (36) performed a chemical and morphological comparison of Aβ peptides and amyloid plaques present in the brains of APP23 transgenic mice and human AD patients. They reported that the amyloid plaques characteristic of AD contain cores that are highly resistant to chemical and physical disruption. In contrast, APP23 mice produced amyloid cores that were completely soluble in buffers containing SDS.

We observed that FAD42 mice have elevated $A\beta_{pE3-x}$ in TBS- and SDS-soluble brain preparations in comparison to TBA42 and 5XFAD mice. The apparent differences between $A\beta_{x-42}$ and $A\beta_{pE3-x}$ levels are likely due to the fact that the $A\beta_{x-42}$ peptides are ~1000-times more abundant than $A\beta_{pE3-x}$. Such a discrepancy was observed previously (21). We hypothesize that $A\beta_{pE3-42}$ elevation does not necessarily lead to increased aggregation of total Aβ if there is already a saturation effect caused by $A\beta_{x-42}$.

$A\beta_{pE3}$ isoforms have been identified by several groups in AD brains (12, 13, 15, 36, 42–52). N-terminal deletions generally enhance aggregation of β-amyloid peptides *in vitro* (53). Additionally, $A\beta_{pE3}$ is known to have a high aggregation propensity (54, 55), increased stability (56), enhanced toxicity compared with full-length Aβ (57), and dramatically reduced solubility at physiological pH-conditions (58). Our findings go along with the $A\beta_{pE3}$ seeding hypothesis (20, 54, 57). Here, we further corroborate the importance of $A\beta_{pE3-42}$ in the etiology of AD by demonstrating the effects of elevating $A\beta_{pE3-42}$ in 5XFAD mice.

Acknowledgments—We thank Petra Tucholla for technical support.

REFERENCES

1. Selkoe, D. J. (1998) The cell biology of β-amyloid precursor protein and presenilin in Alzheimer disease. *Trends Cell Biol.* **8,** 447–453
2. Masters, C. L., Simms, G., Weinman, N. A., Multhaup, G., McDonald, B. L., and Beyreuther, K. (1985) Amyloid plaque core protein in Alzheimer disease and down syndrome. *Proc. Natl. Acad. Sci.* **82,** 4245–4249
3. Miller, D. L., Papayannopoulos, I. A., Styles, J., Bobin, S. A., Lin, Y. Y., Biemann, K., and Iqbal, K. (1993) Peptide compositions of the cerebrovascular and senile plaque core amyloid deposits of Alzheimer disease. *Arch. Biochem. Biophys.* **301,** 41–52
4. Prelli, F., Castaño, E., Glenner, G. G., and Frangione, B. (1988) Differences between vascular and plaque core amyloid in Alzheimer disease. *J. Neurochem.* **51,** 648–651
5. Pike, C. J., Cummings, B. J., and Cotman, C. W. (1995) Early association of reactive astrocytes with senile plaques in Alzheimer disease. *Exp. Neurol.* **132,** 172–179
6. Iwatsubo, T., Odaka, A., Suzuki, N., Mizusawa, H., Nukina, N., and Ihara, Y. (1994) Visualization of Aβ 42(43) and Aβ 40 in senile plaques with end-specific Aβ monoclonals: Evidence that an initially deposited species is Aβ 42(43). *Neuron* **13,** 45–53
7. Barrow, C. J., and Zagorski, M. G. (1991) Solution structures of β peptide and its constituent fragments: Relation to amyloid deposition. *Science* **253,** 179–182
8. Saito, T., Suemoto, T., Brouwers, N., Sleegers, K., Funamoto, S., Mihira, N., Matsuba, Y., Yamada, K., Nilsson, P., Takano, J., Nishimura, M., Iwata, N., Van Broeckhoven, C., Ihara, Y., and Saido, T. C. (2011) Potent amyloidogenicity and pathogenicity of Aβ43. *Nat. Neurosci.* **14,** 1023–1032
9. Welander, H., Frånberg, J., Graff, C., Sundström, E., Winblad, B., and Tjernberg, L. O. (2009) Aβ43 is more frequent than Aβ40 in amyloid plaque cores from Alzheimer disease brains. *J. Neurochem.* **110,** 697–706
10. Näslund, J., Schierhorn, A., Hellman, U., Lannfelt, L., Roses, A. D., Tjernberg, L. O., Silberring, J., Gandy, S. E., Winblad, B., and Greengard, P. (1994) Relative abundance of Alzheimer Aβ amyloid peptide variants in Alzheimer disease and normal aging. *Proc. Natl. Acad. Sci.* **91,** 8378–8382
11. Roher, A. E., Lowenson, J. D., Clarke, S., Woods, A. S., Cotter, R. J., Gowing, E., and Ball, M. J. (1993) β-Amyloid-(1–42) is a major component of cerebrovascular amyloid deposits: Implications for the pathology of Alzheimer disease. *Proc. Natl. Acad. Sci.* **90,** 10836–10840
12. Saido, T. C., Iwatsubo, T., Mann, D. M., Shimada, H., Ihara, Y., and Kawashima, S. (1995) Dominant and differential deposition of distinct β-amyloid peptide species, Aβ N3(pE), in senile plaques. *Neuron* **14,** 457–466
13. Harigaya, Y., Saido, T. C., Eckman, C. B., Prada, C. M., Shoji, M., and Younkin, S. G. (2000) Amyloid β protein starting pyroglutamate at position 3 is a major component of the amyloid deposits in the Alzheimer disease brain. *Biochem. Biophys. Res. Commun.* **276,** 422–427
14. Portelius, E., Bogdanovic, N., Gustavsson, M. K., Volkmann, I., Brinkmalm, G., Zetterberg, H., Winblad, B., and Blennow, K. (2010) Mass spectrometric characterization of brain amyloid β isoform signatures in familial and sporadic Alzheimer disease. *Acta Neuropathol.* **120,** 185–193
15. Güntert, A., Döbeli, H., and Bohrmann, B. (2006) High sensitivity analysis of amyloid-β peptide composition in amyloid deposits from human and PS2APP mouse brain. *Neuroscience* **143,** 461–475
16. Sevalle, J., Amoyel, A., Robert, P., Fournié-Zaluski, M. C., Roques, B., and Checler, F. (2009) Aminopeptidase A contributes to the N-terminal truncation of amyloid β-peptide. *J. Neurochem.* **109,** 248–256
17. Cynis, H., Schilling, S., Bodnár, M., Hoffmann, T., Heiser, U., Saido, T. C., and Demuth, H. U. (2006) Inhibition of glutaminyl cyclase alters pyroglutamate formation in mammalian cells. *Biochim. Biophys. Acta* **1764,** 1618–1625
18. Schilling, S., Hoffmann, T., Manhart, S., Hoffmann, M., and Demuth, H. U. (2004) Glutaminyl cyclases unfold glutamyl cyclase activity under mild acid conditions. *FEBS Lett.* **563,** 191–196
19. Wirths, O., Breyhan, H., Cynis, H., Schilling, S., Demuth, H. U., and Bayer, T. A. (2009) Intraneuronal pyroglutamate-Aβ 3–42 triggers neurodegeneration and lethal neurological deficits in a transgenic mouse model. *Acta Neuropathol.* **118,** 487–496
20. Alexandru, A., Jagla, W., Graubner, S., Becker, A., Bäuscher, C., Kohlmann, S., Sedlmeier, R., Raber, K. A., Cynis, H., Rönicke, R., Reymann, K. G., Petrasch-Parwez, E., Hartlage-Rübsamen, M., Waniek, A., Rossner, S., Schilling, S., Osmand, A. P., Demuth, H. U., and von Hörsten, S. (2011) Selective hippocampal neurodegeneration in transgenic mice expressing small amounts of truncated Aβ is induced by pyroglutamate-Aβ formation. *J. Neurosci.* **31,** 12790–12801
21. Jawhar, S., Wirths, O., Schilling, S., Graubner, S., Demuth, H. U., and Bayer, T. A. (2011) Overexpression of glutaminyl cyclase, the enzyme responsible for pyroglutamate Aβ formation, induces behavioral deficits, and glutaminyl cyclase knock-out rescues the behavioral phenotype in 5XFAD mice. *J. Biol. Chem.* **286,** 4454–4460
22. Schilling, S., Zeitschel, U., Hoffmann, T., Heiser, U., Francke, M., Kehlen, A., Holzer, M., Hutter-Paier, B., Prokesch, M., Windisch, M., Jagla, W., Schlenzig, D., Lindner, C., Rudolph, T., Reuter, G., Cynis, H., Montag, D., Demuth, H. U., and Rossner, S. (2008) Glutaminyl cyclase inhibition attenuates pyroglutamate Aβ and Alzheimer disease-like pathology. *Nat. Med.* **14,** 1106–1111
23. Oakley, H., Cole, S. L., Logan, S., Maus, E., Shao, P., Craft, J., Guillozet-Bongaarts, A., Ohno, M., Disterhoft, J., Van Eldik, L., Berry, R., and Vassar, R. (2006) Intraneuronal β-amyloid aggregates, neurodegeneration, and neuron loss in transgenic mice with five familial Alzheimer disease mutations: Potential factors in amyloid plaque formation. *J. Neurosci.* **26,** 10129–10140
24. Jawhar, S., Trawicka, A., Jenneckens, C., Bayer, T. A., and Wirths, O. (2012) Motor deficits, neuron loss, and reduced anxiety coinciding with axonal degeneration and intraneuronal Aβ aggregation in the 5XFAD mouse model of Alzheimer's disease. *Neurobiol. Aging* **33,** 196.e29–196.e40
25. Wirths, O., Breyhan, H., Schäfer, S., Roth, C., and Bayer, T. A. (2008)

Deficits in working memory and motor performance in the APP/PS1ki mouse model for Alzheimer disease. *Neurobiol. Aging* **29,** 891–901
26. Wirths, O., Bethge, T., Marcello, A., Harmeier, A., Jawhar, S., Lucassen, P. J., Multhaup, G., Brody, D. L., Esparza, T., Ingelsson, M., Kalimo, H., Lannfelt, L., and Bayer, T. A. (2010) Pyroglutamate Aβ pathology in APP/PS1KI mice, sporadic and familial Alzheimer disease cases. *J. Neural Transm.* **117,** 85–96
27. Ida, N., Hartmann, T., Pantel, J., Schröder, J., Zerfass, R., Förstl, H., Sandbrink, R., Masters, C. L., and Beyreuther, K. (1996) Analysis of heterogeneous A4 peptides in human cerebrospinal fluid and blood by a newly developed sensitive Western blot assay. *J. Biol. Chem.* **271,** 22908–22914
28. Portelius, E., Zhang, B., Gustavsson, M. K., Brinkmalm, G., Westman-Brinkmalm, A., Zetterberg, H., Lee, V. M., Trojanowski, J. Q., and Blennow, K. (2009) Effects of gamma-secretase inhibition on the amyloid beta isoform pattern in a mouse model of Alzheimer's disease. *Neurodeg. Dis.* **6,** 258–262
29. Portelius, E., Tran, A. J., Andreasson, U., Persson, R., Brinkmalm, G., Zetterberg, H., Blennow, K., and Westman-Brinkmalm, A. (2007) Characterization of amyloid beta peptides in cerebrospinal fluid by an automated immunoprecipitation procedure followed by mass spectrometry. *J. Prot. Res.* **6,** 4433–4439
30. Harris, J. A., Devidze, N., Verret, L., Ho, K., Halabisky, B., Thwin, M. T., Kim, D., Hamto, P., Lo, I., Yu, G. Q., Palop, J. J., Masliah, E., and Mucke, L. (2010) Trans-synaptic progression of amyloid-β-induced neuronal dysfunction within the entorhinal-hippocampal network. *Neuron* **68,** 428–441
31. Awadé, A. C., Cleuziat, P., GonzalèS, T., and Robert-Baudouy, J. (1994) *Proteins: Structure, Function, and Genetics,* Vol. 20, pp. 34–51, Wiley-Liss, New York
32. Cynis, H., Hoffmann, T., Friedrich, D., Kehlen, A., Gans, K., Kleinschmidt, M., Rahfeld, J. U., Wolf, R., Wermann, M., Stephan, A., Haegele, M., Sedlmeier, R., Graubner, S., Jagla, W., Müller, A., Eichentopf, R., Heiser, U., Seifert, F., Quax, P. H., de Vries, M. R., Hesse, I., Trautwein, D., Wollert, U., Berg, S., Freyse, E. J., Schilling, S., and Demuth, H. U. (2011) The isoenzyme of glutaminyl cyclase is an important regulator of monocyte infiltration under inflammatory conditions. *EMBO Mol. Med.* **3,** 545–558
33. Galimberti, D., Fenoglio, C., Lovati, C., Venturelli, E., Guidi, I., Corrà, B., Scalabrini, D., Clerici, F., Mariani, C., Bresolin, N., and Scarpini, E. (2006) Serum MCP-1 levels are increased in mild cognitive impairment and mild Alzheimer disease. *Neurobiol. Aging* **27,** 1763–1768
34. Casas, C., Sergeant, N., Itier, J. M., Blanchard, V., Wirths, O., van der Kolk, N., Vingtdeux, V., van de Steeg, E., Ret, G., Canton, T., Drobecq, H., Clark, A., Bonici, B., Delacourte, A., Benavides, J., Schmitz, C., Tremp, G., Bayer, T. A., Benoit, P., and Pradier, L. (2004) Massive CA1/2 neuronal loss with intraneuronal and N-terminal truncated Aβ42 accumulation in a novel Alzheimer transgenic model. *Am. J. Pathol.* **165,** 1289–1300
35. Kawarabayashi, T., Younkin, L., Saido, T., Shoji, M., Ashe, K., and Younkin, S. (2001) Age-dependent changes in brain, CSF, and plasma amyloid (β) protein in the Tg2576 transgenic mouse model of Alzheimer disease. *J. Neurosci.* **21,** 372–381
36. Kuo, Y. M., Kokjohn, T. A., Beach, T. G., Sue, L. I., Brune, D., Lopez, J. C., Kalback, W. M., Abramowski, D., Sturchler-Pierrat, C., Staufenbiel, M., and Roher, A. E. (2001) Comparative analysis of amyloid-β chemical structure and amyloid plaque morphology of transgenic mouse and Alzheimer disease brains. *J. Biol. Chem.* **276,** 12991–12998
37. Maeda, J., Ji, B., Irie, T., Tomiyama, T., Maruyama, M., Okauchi, T., Staufenbiel, M., Iwata, N., Ono, M., Saido, T. C., Suzuki, K., Mori, H., Higuchi, M., and Suhara, T. (2007) Longitudinal, quantitative assessment of amyloid, neuroinflammation, and anti-amyloid treatment in a living mouse model of Alzheimer disease enabled by positron emission tomography. *J. Neurosci.* **27,** 10957–10968
38. Christensen, D. Z., Kraus, S. L., Flohr, A., Cotel, M. C., Wirths, O., and Bayer, T. A. (2008) Transient intraneuronal Aβ rather than extracellular plaque pathology correlates with neuron loss in the frontal cortex of APP/PS1KI mice. *Acta Neuropathol.* **116,** 647–655
39. Wirths, O., Erck, C., Martens, H., Harmeier, A., Geumann, C., Jawhar, S., Kumar, S., Multhaup, G., Walter, J., Ingelsson, M., Degerman-Gunnarsson, M., Kalimo, H., Huitinga, I., Lannfelt, L., and Bayer, T. A. (2010) Identification of low molecular weight pyroglutamate Aβ oligomers in Alzheimer Disease – a novel tool for therapy and diagnosis. *J. Biol. Chem.* **285,** 41517–41524
40. Christensen, D. Z., Bayer, T. A., and Wirths, O. (2010) Intracellular Aβ triggers neuron loss in the cholinergic system of the APP/PS1KI mouse model of Alzheimer disease. *Neurobiol. Aging* **31,** 1153–1163
41. Bayer, T. A., and Wirths, O. (2010) *Front. Aging Neurosci.* **10,** 2–8
42. Russo, C., Saido, T. C., DeBusk, L. M., Tabaton, M., Gambetti, P., and Teller, J. K. (1997) Heterogeneity of water-soluble amyloid β-peptide in Alzheimer disease and Down syndrome brains. *FEBS Lett.* **409,** 411–416
43. Piccini, A., Zanusso, G., Borghi, R., Noviello, C., Monaco, S., Russo, R., Damonte, G., Armirotti, A., Gelati, M., Giordano, R., Zambenedetti, P., Russo, C., Ghetti, B., and Tabaton, M. (2007) Association of a presenilin 1 S170F mutation with a novel Alzheimer disease molecular phenotype. *Arch. Neurol.* **64,** 738–745
44. Mori, H., Takio, K., Ogawara, M., and Selkoe, D. J. (1992) Mass spectrometry of purified amyloid β protein in Alzheimer disease. *J. Biol. Chem.* **267,** 17082–17086
45. Saido, T. C., Yamao-Harigaya, W., Iwatsubo, T., and Kawashima, S. (1996) Amino- and carboxyl-terminal heterogeneity of β-amyloid peptides deposited in human brain. *Neurosci. Lett.* **215,** 173–176
46. Kuo, Y. M., Emmerling, M. R., Woods, A. S., Cotter, R. J., and Roher, A. E. (1997) Isolation, chemical characterization, and quantitation of Aβ 3-pyroglutamyl peptide from neuritic plaques and vascular amyloid deposits. *Biochem. Biophys. Res. Commun.* **237,** 188–191
47. Hosoda, R., Saido, T. C., Otvos, L., Jr., Arai, T., Mann, D. M., Lee, V. M., Trojanowski, J. Q., and Iwatsubo, T. (1998) Quantification of modified amyloid β peptides in Alzheimer disease and Down syndrome brains. *J. Neuropathol. Exp. Neurol.* **57,** 1089–1095
48. Iwatsubo, T., Saido, T. C., Mann, D. M., Lee, V. M., and Trojanowski, J. Q. (1996) Full-length amyloid-β (1–42(43)) and amino-terminally modified and truncated amyloid-β 42(43) deposit in diffuse plaques. *Am. J. Pathol.* **149,** 1823–1830
49. Miravalle, L., Calero, M., Takao, M., Roher, A. E., Ghetti, B., and Vidal, R. (2005) Amino-terminally truncated Aβ peptide species are the main component of cotton wool plaques. *Biochemistry* **44,** 10810–10821
50. Piccini, A., Russo, C., Gliozzi, A., Relini, A., Vitali, A., Borghi, R., Giliberto, L., Armirotti, A., D'Arrigo, C., Bachi, A., Cattaneo, A., Canale, C., Torrassa, S., Saido, T. C., Markesbery, W., Gambetti, P., and Tabaton, M. (2005) β-Amyloid is different in normal aging and in Alzheimer disease. *J. Biol. Chem.* **280,** 34186–34192
51. Tekirian, T. L., Saido, T. C., Markesbery, W. R., Russell, M. J., Wekstein, D. R., Patel, E., and Geddes, J. W. (1998) N-terminal heterogeneity of parenchymal and cerebrovascular Aβ deposits. *J. Neuropathol. Exp. Neurol.* **57,** 76–94
52. Jawhar, S., Wirths, O., and Bayer, T. A. (2011) Pyroglutamate amyloid-β (Aβ): A hatchet man in Alzheimer disease. *J. Biol. Chem.* **286,** 38825–38832
53. Pike, C. J., Overman, M. J., and Cotman, C. W. (1995) Amino-terminal deletions enhance aggregation of β-amyloid peptides *in vitro*. *J. Biol. Chem.* **270,** 23895–23898
54. He, W., and Barrow, C. J. (1999) The Aβ 3-pyroglutamyl and 11-pyroglutamyl peptides found in senile plaque have greater β-sheet forming and aggregation propensities *in vitro* than full-length Aβ. *Biochemistry.* **38,** 10871–10877
55. Schilling, S., Lauber, T., Schaupp, M., Manhart, S., Scheel, E., Böhm, G., and Demuth, H. U. (2006) On the seeding and oligomerization of pGlu-amyloid peptides (*in vitro*). *Biochemistry.* **45,** 12393–12399
56. Kuo, Y. M., Webster, S., Emmerling, M. R., De Lima, N., and Roher, A. E. (1998) Irreversible dimerization/tetramerization and post-translational modifications inhibit proteolytic degradation of Aβ peptides of Alzheimer disease. *Biochim. Biophys. Acta* **1406,** 291–298
57. Russo, C., Violani, E., Salis, S., Venezia, V., Dolcini, V., Damonte, G., Benatti, U., D'Arrigo, C., Patrone, E., Carlo, P., and Schettini, G. (2002) Pyroglutamate-modified amyloid β-peptides–AβN3(pE)–strongly affect cultured neuron and astrocyte survival. *J. Neurochem.* **82,** 1480–1489
58. Schlenzig, D., Manhart, S., Cinar, Y., Kleinschmidt, M., Hause, G., Willbold, D., Funke, S. A., Schilling, S., and Demuth, H. U. (2009) Pyroglutamate formation influences solubility and amyloidogenicity of amyloid peptides. *Biochemistry* **48,** 7072–7078